INL/CON-09-15462
PREPRINT

# Effect of Channel Configurations for Tritium Transfer in Printed Circuit Heat Exchangers

## ICAPP '09

Chang Oh
Eung Kim
Robert Shrake
Mike Patterson

May 2009

The INL is a
U.S. Department of Energy
National Laboratory
operated by
Battelle Energy Alliance

Proceedings of ICAPP '09
Tokyo, Japan, May 10-14, 2009
Paper 9146

# EFFECT OF CHANNEL CONFIGURATIONS FOR TRITIUM TRANSFER IN PRINTED CIRCUIT HEAT EXCHANGERS

Chang Oh, Eung Kim, Robert Shrake, and Mike Patterson
*Idaho National Laboratory*
*P.O. Box 1625*
*Idaho Falls, ID 83415*
*Tel:208-526-7716 , Fax:208-526-0528, Email:Chang.Oh@inl.gov*

Abstract –*The Next Generation Nuclear Plant (NGNP), a very High temperature Gas-Cooled Reactor (VHTR) concept, will provide the first demonstration of a closed-loop Brayton cycle at a commercial scale of a few hundred megawatts electric and hydrogen production. The power conversion system (PCS) for the NGNP will take advantage of the significantly higher reactor outlet temperatures of the VHTR to provide higher efficiencies than can be achieved in the current generation of light water reactors. Besides demonstrating a system design that can be used directly for subsequent commercial deployment, the NGNP will demonstrate key technology elements that can be used in subsequent advanced power conversion systems for other Generation IV reactors. In anticipation of the design, development and procurement of an advanced power conversion system for the NGNP, the system integration of the NGNP and hydrogen plant was initiated to identify the important design and technology options that must be considered in evaluating the performance of the proposed NGNP.*

*In the VHTR system, an intermediate heat exchanger (IHX), which transfers heat from the reactor core to the electricity or hydrogen production system is one key component, and its effectiveness is directly related to the system overall efficiency. In the VHTRs, the gas fluids used for coolant generally have poor heat transfer capability, so it requires very large surface area for a given condition. For this reason, a compact heat exchanger (CHE), which is widely used in industry especially for gas-to-gas or gas-to-liquid heat exchange is considered as a potential candidate for an IHX replacing the classical shell and tube type heat exchanger. A compact heat exchanger is arbitrary referred to be a heat exchanger having a surface area density greater than 700 $m^2/m^3$. The compactness is usually achieved by fins and micro-channels, and leads to the enormous heat transfer enhancement and size reduction. The surface area density is the total heat transfer area divided by the volume of the heat exchanger. In the case of PCHE units, the heat transfer surface area density may be as high as 2,500 $m^2/m^3$. This high compactness implies an appreciable reduction in material reducing cost.*

*In this study, heat transfer and tritium penetration analyses have been performed for two different channel configurations of the PCHE; (1) standard and (2) off-set. One of the goals of this study was to determine whether offsetting the hot and cold streams would significantly reduce the tritium flux, and whether or not it would affect the heat transfer significantly.*

## I. INTRODUCTION

The U.S. Department of Energy is working through the Idaho National Laboratory to explore the potential for a Next Generation Nuclear Plant (NGNP) [1] based on the Very High Temperature Gas-Cooled Reactor (VHTR). The candidate system may be either a pebble-bed or a prismatic, graphite-moderated thermal neutron-spectrum reactor using helium as the working fluid. Presently the reactor outlet temperature has not been specified. However, dependent on the NGNP mission, the design average outlet temperature may be as high as 950 ºC (1223 K).

Because the NGNP may be used to generate process heat an intermediate heat exchanger will likely be a part of the primary system. Also, because the NGNP will likely be used to generate electricity, the plant may be either a direct-cycle or an indirect cycle system. The Brayton cycle may be used to generate electricity. The reactor will be designed to ensure passive decay heat removal without fuel damage throughout the accident envelope.

The basic technology for the NGNP has been established in former high-temperature gas-cooled reactor plants (e.g., DRAGON, Peach Bottom, Albeitsgemeinschaft Versuchsreaktor [AVR], Thorium Hochtemperatur Reaktor [THTR], and Fort St. Vrain [2]). These reactor designs represent the two design categories: the pebble bed reactor

and the prismatic modular reactor. Commercial examples of potential NGNP candidates are the Gas Turbine-Modular Helium Reactor (GT-MHR) from General Atomics [3], the High Temperature Reactor concept from AREVA [4], and the Pebble Bed Modular Reactor (PBMR) from the PBMR consortium [5]. Furthermore, the Japanese High-Temperature Engineering Test Reactor (HTTR) and the Chinese High-Temperature Reactor (HTR-10) are demonstrating the feasibility of the reactor components and materials needed for the NGNP. (The HTTR achieved a maximum average coolant outlet temperature of 950°C (1223 K) in April, 2004.) Therefore, the NGNP program is focused on building a plant to publicly demonstrate the safety and economics of the VHTR, rather than simply confirming the basic feasibility of the concept.

## II. COMSOL MODELING

In this work, in order to compare the performance of heat transfer and tritium penetration in the PCHEs, the analysis was performed using COMSOL Multiphysics 3.4 [6]. The COMSOL Multiphysics (formerly FEMLAB) software is a finite element analysis and solver software package for various physics and engineering applications, especially coupled phenomena, or multiphysics. This software offers several application-specific modules including electromagnetic, acoustic, chemical engineering, earth science, heat transfer, fluid dynamics, structure mechanics models and etc. Besides these, it also allows for entering coupled systems of partial differential equations (PDEs). The PDEs can be entered directly or using weak forms. In this work, simple heat transfer and diffusion modules were used for PCHE [7] analysis.

### *Geometry and Dimensions*

Figure 1 shows the PCHE channel configurations used here; (1) standard in-line and (2) off-set. Originally, a PCHE has a standard in-line configuration, but in this work, the off-set configuration was also considered as an alternative. The reference PCHE configuration had a plate thickness of 0.96mm ($t_p$=0.96mm) and a pitch of 1.464mm (p=1.464mm). The diameter of the semicircular ports was 1.2mm ($d_t$=1.2mm). Calculations were performed for five horizontal pitches (1.332mm, 1.464mm, 1.728mm, 1.992mm, and 2.5mm) and five plate thicknesses (0.69mm, 0.96mm, 1.32mm, 2.54mm, and 3.48mm).The horizontal pitch, plate thickness, and diameter are shown on Figure 1. The offset model was made by shifting every other plate by half the model's pitch.

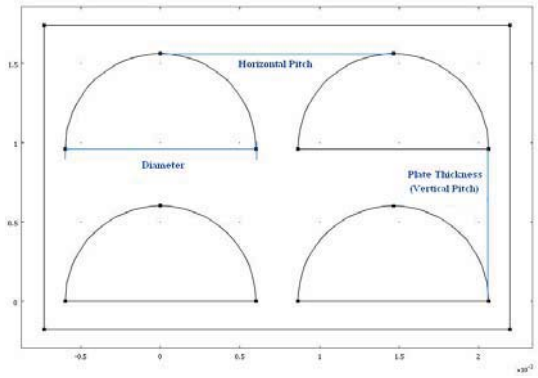


(a) Stand in-line configuration.

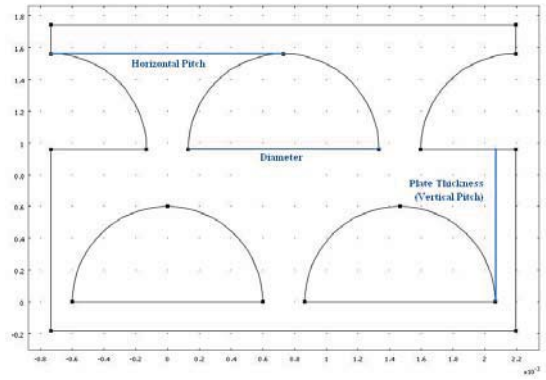


(b) Off-set configuration.

Figure 1. PCHE channel configurations.

### *Properties and Boundary Conditions*

In this work, the heat transfer and mass diffusion equations were solved in the PCHE solid region, but they were not solved in the fluid region. In the fluid region, simple convective heat and mass transfer correlations were used in order to determine the boundary temperatures and tritium concentrations on the solid surface. For analysis, the data for Alloy 800 was implemented into the model because of the lack of Alloy 617 data for the tritium diffusion. Since the purpose of this study is to compare the performance of different channel configurations, the results from Alloy 800 are still valid for other metals such as Alloy 617 or 230. The following diffusion coefficient was used for tritium permeation calculation [8].

$$D_{tritium} = 61.02 \cdot \sqrt{\frac{P}{C_{H_2}}} \cdot \exp(-\frac{6250}{T})$$

where,

$D_{tritium}$ = diffusion coefficient of tritium in Alloy 800

$P$ = pressure (atm)

$C_{H_2}$ = hydrogen concentration (ppmv)

$T$ = temperature (K)

As mentioned above, the boundary conditions for the heat transfer and mass transfer were determined by convective heat/mass transfer correlations. In order to consider this, Schmidt number (Sc), $k_{diffusion}$, and the diffusion coefficient were calculated based on the bulk conditions of the fluid assumed by the VHTR IHX conditions [9, 10]. The assumed Reynolds numbers (Re) in the hot channel and cold channel are 2800 and 2200, respectively. The following equations were selected for determinations of heat transfer and diffusion boundary conditions [11].

(a) Heat Transfer

$$\frac{h_{convective} \cdot d_h}{k_{therm}} = 0.023 \cdot \mathrm{Re}^{0.83}\, Sc^{0.44}$$

(b) Tritium Diffusion

$$\frac{K_{diffusion} \cdot d_h}{D_{tritium}} = 0.023 \cdot \mathrm{Re}^{0.83}\, Sc^{0.44}$$

The analysis was performed with a number of different boundary conditions. The following boundary conditions were used (slightly modified from the Ref [12]). As shown below, for tritium permeation analysis, the bulk temperatures in the fluid channels were matched to be the same for eliminating the effect of temperature gradient.

*Tritium Concentration in the Bulk Fluids*
- Primary Coolant Tritium Concentration: 115 μCi/m$^3$
- Secondary Coolant Tritium Concentration: 113 μCi/m$^3$
- Primary Coolant Hydrogen Concentration: 200 ppm

*Temperatures in the Bulk Fluids*
*a. For heat transfer analysis*
- Primary Coolant Inlet T: 900 deg. C
- Primary Coolant Inlet P: 69.08 atm (7 MPa)
- Secondary Coolant Outlet T: 886.3 deg. C
- Secondary Coolant Outlet P: 68.59 atm (6.95 MPa)

- Primary Coolant Outlet T: 495.5 deg. C
- Primary Coolant Outlet P: 68.59 atm (6.95 MPa)
- Secondary Coolant Inlet T: 486.3 deg. C
- Secondary Coolant Inlet P: 69.08 atm (7 MPa)

*a. For tritium permeation analysis*
- Primary Coolant T: 500 C
- Primary Coolant P: 69.08 atm (7 MPa)
- Secondary Coolant T: 500 deg. C
- Secondary Coolant P: 69.08 atm (7 MPa)

- Primary Coolant T: 600 C
- Primary Coolant P: 69.08 atm (7MPa)
- Secondary Coolant T: 600 deg. C
- Secondary Coolant P: 69.08 atm (7MPa)

- Primary Coolant T: 700 C
- Primary Coolant P: 69.08 atm (7MPa)
- Secondary Coolant T: 700 deg. C
- Secondary Coolant P: 69.08 atm (7MPa)

- Primary Coolant T: 800 C
- Primary Coolant P: 69.08 atm (7MPa)
- Secondary Coolant T: 800 deg. C
- Secondary Coolant P: 69.08 atm (7MPa)

- Primary Coolant T: 900 C
- Primary Coolant P: 69.08 atm (7MPa)
- Secondary Coolant T: 900 deg. C
- Secondary Coolant P: 69.08 atm (7MPa)

The outer boundary conditions of the COMSOL models were set to be periodic, so flux calculations assume an infinite array of hot and cold ports, and don't take into account the difference in flux at the sides of the heat exchanger. There are approximately 200,000 ports in the PCHE being considered for the NGNP, so the error associated with this assumption is considered to be minimal.

***Method of Grid Sensitivity Study***

The mesh or grid size is very important issue in the CFD or FEM code analysis, because it highly affects the quantitative results of the simulations. Generally, the grid is refined and the time step is refined, the spatial and temporal discretization errors should asymptotically approach zero, excluding computer round-off error.

In this work, we followed the grid sensitivity analysis procedure proposed for validation and verification of CFD codes by the Ref. [13]. Since the basic concept of the grid sensitivity study is based on the Richardson extrapolation methods, the guideline used in CFD codes are still valid for FEM codes. The followings are the summary of the grid sensitivity study in the "NPARC Alliance CFD Verification and Validation" website in NASA.

***a. Grid Consideration for a Grid Convergence Study***

In generating the fine grid, one can build in the n levels of coarser grids by making sure that the number of grid points in each coordinate direction satisfies the relation

$$N = 2^n m + 1$$

For example, if two levels of coarser grids are desired (i.e. fine, medium and coarse grids) than the number of grid points in each coordinate direction must equal 4m+1. The m may be different for each coordinate direction.

It is not necessary to halve the number of grid points in each coordinate direction to obtain the coarse grid. But it is important to maintain the same grid generation parameters as the original grid.

***b. Order of Grid Convergence***

The order of grid convergence involves the behavior of the solution error defined as the difference between the discrete solution and the exact solution,

$$E = f(h) - f_{exact} = Ch^P + H.O.T$$

Where C is a constant, h is some measure of grid spacing, and p is the order of convergence. A "second-order" solution would have p=2.

Neglecting higher-order terms and taking the logarithm of both sides of the above equation results in

$$\log(E) = \log(C) + p\,\log(h)$$

The order of convergence p can be obtained from the slope of the curve of log (E) versus log (h).

A more direct evaluation of p can be obtained from three solutions using a constant grid refinement ratio r,

$$p = \ln\left(\frac{f_3 - f_2}{f_2 - f_1}\right) / \ln(r)$$

The order of accuracy is determined by the order of the leading term of the truncation error and is represented with respect to the scale of the discretization, h. The local order of accuracy is the order for the stencil representing the discretization of the equation at one location in the grid. The global order of accuracy considers the propagation and accumulation of errors outside the stencil. This propagation causes the global order of accuracy to be, in general, one degree less than the local order of accuracy. The order of accuracy of the boundary conditions can be one order of accuracy lower than the interior order of accuracy without degrading the overall global accuracy.

***c. Asymptotic Range of Convergence***

Assessing the accuracy of code and calculations requires that the grid is sufficiently refined such that the solution is in the asymptotic range of convergence. The asymptotic range of convergence is obtained when the grid spacing is such that the various grid spacing h and errors E result in the constancy of C,

$$C = E / h^p$$

***d. Richardson Extrapolation***

Richardson extrapolation is a method for obtaining a higher-order estimate of the continuum value from a series of lower-order discrete values.

A simulation will yield a quantity f that can be expressed in a general form by the series expansion

$$f = f_{h=0} + g_1 h + g_2 h^2 + g_3 h^3 + \ldots$$

where h is the grid spacing. The quantity f is considered "second-order" if $g_1 = 0.0$. $f_{h=0}$ is the continuum value when the mesh is infinitely small.

If one assumes a second-order solution and has computed f on two grid of spacing h1 and h2 with h1 being the finer spacing, then one can write two equations for the above expansion, neglect third-order and higher terms, and solve for $f_{h=0}$ to estimate the continuum value,

$$f_{h=0} \cong f_1 + \frac{f_1 - f_2}{r^2 - 1}$$

where the grid refinement ratio is

$$f = h_2 / h_1$$

The Richardson extrapolation can be generated for a p-th order methods and r-value of grid ration as

$$f_{h=0} \cong f_1 + \frac{f_1 - f_2}{r^p - 1}$$

Traditionally, Richardson extrapolation has been used with grid refinement ratios of r = 2. Thus, the above equation simplifies to

$$f_{h=0} \cong \frac{4}{3} f_1 - \frac{1}{3} f_2$$

If a larger number of CFD computations are to be performed, one may wish to use the coarser grid with $h_2$. We will then want to estimate the error on the coarser grid. The Richardson extrapolation can be expressed as

$$f_{h=0} \cong f_2 + \frac{(f_1 - f_2) r^p}{r^p - 1}$$

The estimated fractional error for $f_2$ is defined as

$$E_2 = \frac{\varepsilon \cdot r^p}{r^p - 1}$$

Richardson extrapolation is based on a Taylor series representation. If there are shocks and other discontinuities present, the Richardson extrapolation is invalid in the region of the discontinuity.

***e. Grid Convergence Index (GCI)***

Roache suggested a grid convergence index, GCI to provide a consistent manner in reporting the results of grid convergence studies and provide an error band on the grid convergence of the solution.

One significant issue in numerical computation is what level of grid resolution is appropriate. This is a function of flow conditions, type of analysis, geometry, and other variables.

The GCI is a measure of the percentage the computed values are away from the values of the asymptotic numerical value. It indicates an error band on how far the solution is from the asymptotic value. It indicates how much the solution would change with a further refinement of the grid. A small value of the GCI indicates that the computation is within the asymptotic range.

The GCI on the fine grid is defined as

$$GCI_{fine} = \frac{F_s |\varepsilon|}{(r^p - 1)}$$

where Fs is a factor of safety. The refinement may be spatial or in time. The factor of safety is recommended to be Fs = 3.0 for comparisons of two grids and Fs = 1.25 for comparisons over three or more grids. The higher factor of safety is recommended for reporting purposes and is quite conservative of the actual errors.

The GCI for the coarser grid is defined as

$$GCI_{fine} = \frac{F_s |\varepsilon| r^p}{(r^p - 1)}$$

It is important that each grid level yield solution that are in the asymptotic range of convergence for the computed solution. This can be checked by observing two GCI values as computed over three grids,

$$GCI_{23} = r^p GCI_{12}$$

***f. Required Grid Resolution***

If a desired accuracy level is known and results from the grid resolution study are available, one can then estimate the grid resolution required to obtain level of accuracy,

$$r^* = \left( \frac{GCI^*}{GCI_{21}} \right)^{1/p}$$

***g. Effective Grid Refinement Ratio***

If one generates a finer or coarser grid and is unsure of the value of grid refinement ratio to use, one can compute an effective grid refinement ratio as

$$r_{effective} = \left( \frac{N_1}{N_2} \right)^{(1/D)}$$

where N is the total number of grid points used for the grid and D is the dimension of the flow domain. This effective grid refinement ratio can also used for unstructured grids.

III. Results and Discussions

***<u>Heat and Tritium Diffusion Analysis in the PCHEs</u>***

Figures 2 and 3 are a graphical representation of the concentration and temperature profiles using the Primary Inlet Conditions in the two reference configurations (standard and off-set). Analysis of flux data for seven different temperatures and two different pressures showed a 1% decrease in tritium flux and negligible decrease in heat flux when calculated using the reference geometries (horizontal pitch=1.464mm; vertical pitch=0.96mm; diameter=1.2mm The heat flux for the off-set configuration was equal to 99.98% of the initial value for the reference configurations. Flux values were extrapolated to find the value as the mesh size approaches zero using Richardson's method, summarized in the previous section. The error associated with this extrapolation is 1.5% for the initial configuration and 1.7% for the offset configuration when calculating tritium flux.

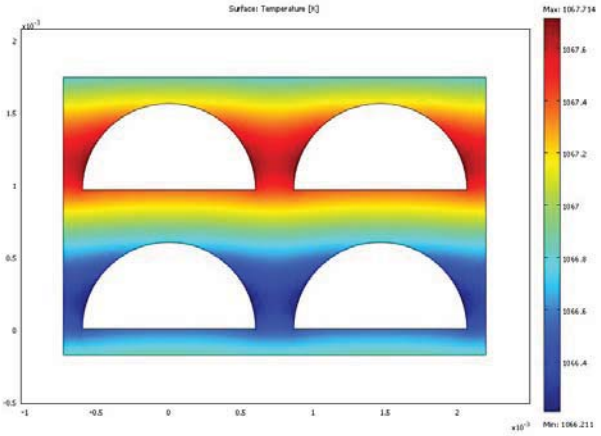

(a) Temperature Profiles

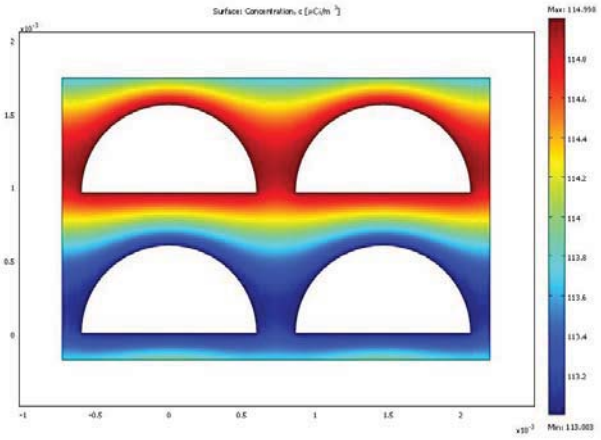

(b) Concentration Profiles

Figure 2. Calculated temperature and tritium concentration profiles (for the standard configuration).

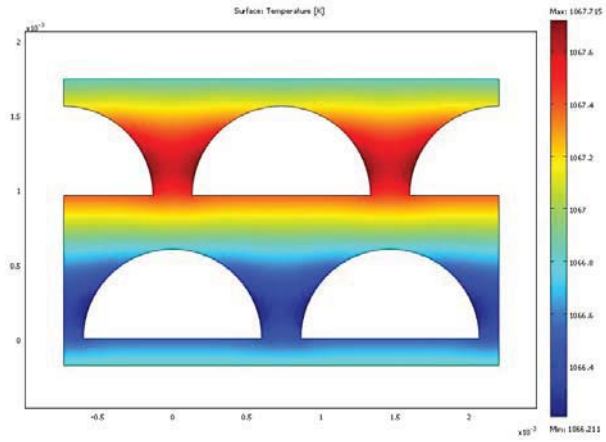

(a) Temperature profile

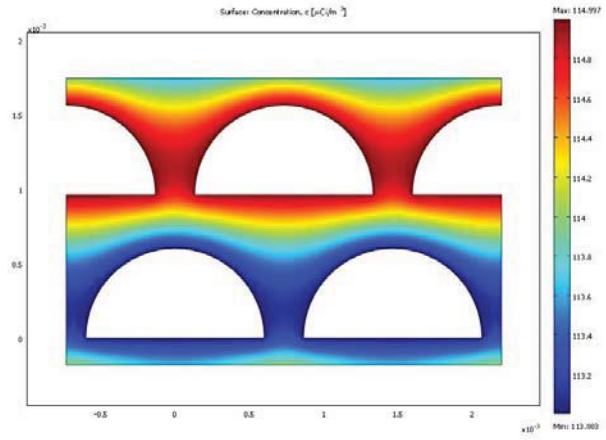

(b) Concentration profile

Figure 3. Calculated temperature and tritium concentration profiles (for the off-set configuration).

This analysis showed the majority of the resistance to heat transfer is found in the fluid boundary layer, not in the metal itself. On the other hand, the majority of resistance to tritium flux is found in the metal itself. Knowing this, the tritium flux can be reduced through the metal without greatly reducing heat transfer.

Figures 4 and 5 show profiles of tritium diffusion flux, and the main penetration paths for standard and off-set configurations, respectively. As shown in these figures, the tritium flux on the flow channel is not uniform along the surface. Most of the tritium diffusion is concentrated on the center part of the semicircle area. On the other hand, there is very small tritium penetration on the channel side because of very small concentration gradient in this direction. The dead spot area is highly dependent on the channel horizontal pitch.

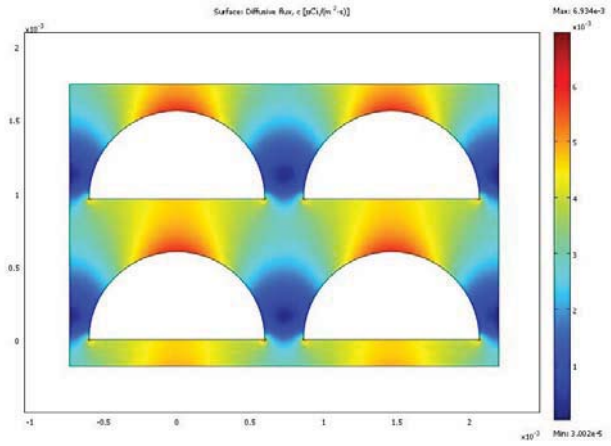

(a) Diffusion flux

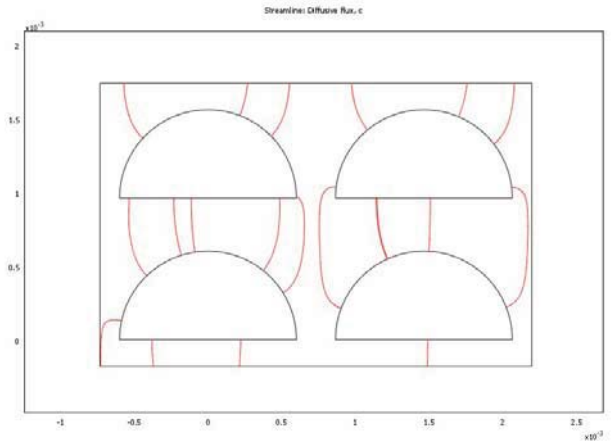

(b) Diffusion path

Figure 4. Diffusion flux and path of tritium in the PHCE (for the standard configuration).

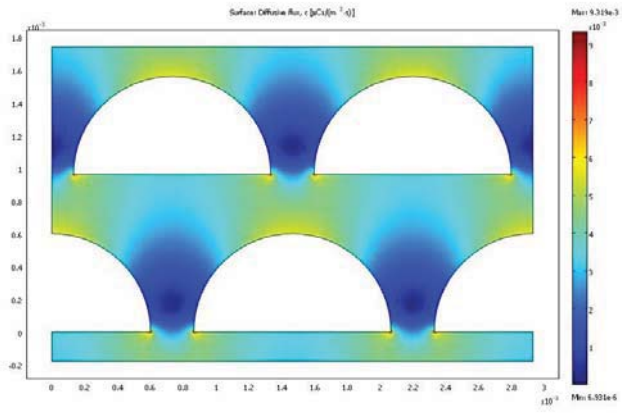

(a) Diffusion flux

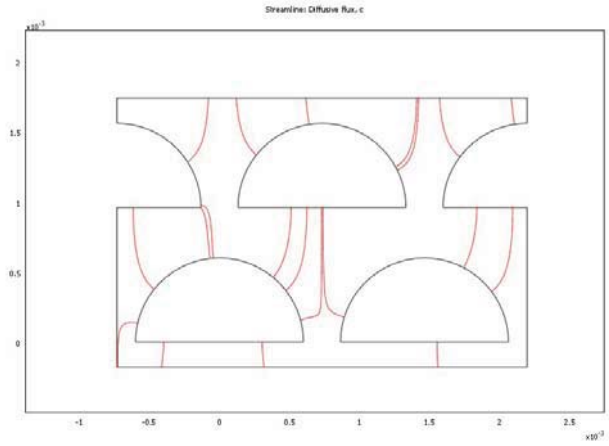

(b) Diffusion path

Figure 5. Diffusion flux and path of tritium in the PHCE (for the off-set configuration).

Figure 6 shows the tritium flux for different horizontal pitches and plate thickness. These calculations represent the flux at the primary coolant inlet side of a counter-current PCHE heat exchanger. As shown in this figure, the tritium penetration flux is significantly decreased by increasing the plate thickness. However, the change of horizontal pitch does not highly affect the tritium penetration flux. According to our calculation, increase of horizontal pitch slightly increases the overall tritium penetration rate by decreasing the dead spot area on the side of the channels.

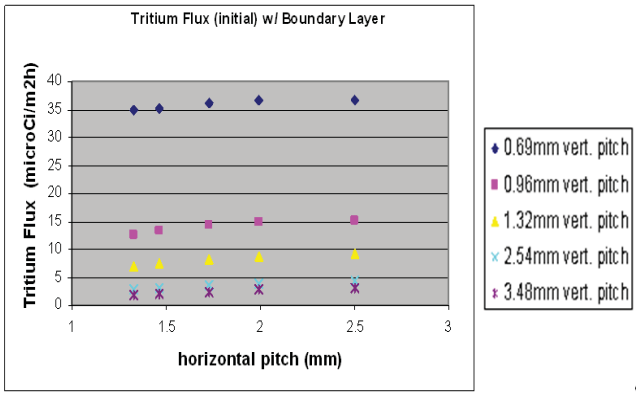


Figure 6. Tritium flux vs. horizontal pitch.

## V. CONCLUSIONS

In this study, heat transfer and tritium penetration analyses have been performed for two different channel configurations of the PCHE; (1) standard and (2) off-set. It was determined that depending on factors like the horizontal and vertical pitch; the off-set configuration can be favorable over the standard configuration. It was seen

that flux is weakly dependent on the horizontal pitch. The flux slowly increases as the horizontal pitch slowly increases. This is because of an increased dead space, as seen in figures 4 and 5. The one exception to this is in the off-set configuration. If the horizontal pitch to vertical pitch ratio is very large, the flux starts to decrease as the horizontal pitch increases. The vertical pitch and flux relationship was much simpler. As the vertical pitch (plate thickness) increases, the flux decreases. This makes sense because there is a longer flux pathway.

The effective thickness of the models was much less than the average thickness. As seen in figures 4 and 5, the majority of the tritium passes through the middle of the models. Therefore, the effective thickness is most similar to the thickness at this location of the model.

Tritium flux was seen to vary widely as the model geometry changed. The majority of the resistance to tritium flux was through the metal, so as the shape of the metal changed, the flux changed respectively. The flux varied from 23.77% to 262.11% of the reference flux value (13.3 $\mu Ci/m^2h$) as the geometry changed.

Heat flux changed much less as the model geometry changed. The majority of the resistance to heat flux was through the helium boundary layer, so as the shape of the metal changed; the flux changed only a little. The heat flux varied from 84.28% to 102.89% of the reference value (149.22 $MW/m^2$) as the geometry changed.

The off-set configuration tended to have slightly less flux for a given horizontal and vertical pitch. This was because the flux pathway tended to be slightly longer, as can be seen in figures 4 and 5. This effect was seen the most when the horizontal pitch was large and the vertical pitch was small, because in this case the flux pathway was almost lateral instead of longitudinal.

## ACKNOWLEDGMENTS

This work was supported through the U.S. Department of Energy's NGNP-Engineering Program under DOE Idaho Operations Office Contract DE-AC07-99ID13727.

## REFERENCES

[1] P.E. Macdonald et al., "The Next Generation Nuclear Plant- Insights gained from the INEEL Point Design Studies," INEEL, INEEL/CON-04-01563, 2004.

[2] NRC, Report to Congress on Abnormal Occurrence, NUREG-0090, Vol. 9, No. 3, April, 1987.

[3] General Atomics, *Gas Turbine-Modular helium Reactor (GT-MHR) Conceptual Design Description Report*, 910720, Revision 1, July, 1996.

[4] F. Southworth, AREVA HTR Development, University of Calgary, November 3, 2006.

[5] D.R. Nicholls, "Status of the Pebble Bed Modular Reactor," *Nuclear Energy* **39**, No.4, 2000.

[6] COMSOL, Inc., Comsol 3.4 Multiphysics user's Guide, 2007.

[7] Heatric™ Workshop at MIT on 2nd October 2003, Cambridge: MA, 2003.

[8] Richards, M. B., Shenoy, A. S., Brown, L. C., Buckingham, R. T., Harvego, E.A., Peddicord, K. L., Reza, S. M. M., Coupey, J. P., Apr. 2006, *H2-MHR Pre-Conceptual Report: SI-Based Plant, General Atomics Report GA-A25401*

[9] C.H. Oh, E.S. Kim, S. Sherman, R. Vilim, R., Y.J. Lee, and W.J. Lee, HyPEP FY-07 Annual Report: A Hydrogen Production Plant Efficiency Calculation Program, INL/EXT-07-13078, 2007

[10] E. Kim, C.H. Oh, and S. Sherman, "Optimum Sizing and Cost Analysis for Compact Heat Exchanger in VHTR," in press in *Nuclear Engineering and Design*,, Vol. 238 (10), October 2008, pp. 2635-2647.

[11] R.H. Perry, D.W. Green, 1997, *Perry's Chemical Engineers' Handbook: 7th Edition*

[12] H. Ohashi, S. Sherman, June 2007, *Tritium Movement and Accumulation in the NGNP System Interface and Hydrogen Plant*

[13] AIAA, "Guide for the Verification and Validation of Computational Fluid Dynamics Simulations," AIAA G-077-1998,